

Electronic structure and Peierls instability in graphene nanoribbons sculpted in graphane

Valentina Tozzini* and Vittorio Pellegrini

NEST, Istituto Nanoscienze–CNR, Scuola Normale Superiore, I-56127 Pisa, Italy

(Received 29 October 2009; revised manuscript received 22 February 2010; published 18 March 2010)

Graphene nanoribbons are semiconductor nanostructures with great potentials in nanoelectronics. Their realization particularly with small lateral dimensions below a few nanometers, however, remains challenging. Here we theoretically analyze zigzag graphene nanoribbons created in a graphane substrate (a fully saturated two-dimensional hydrocarbon with formula CH) and predict that they are stable down to the limit of a single carbon chain. We exploit density functional theory with B3LYP functional that accurately treats exchange and correlation effects and demonstrate that at small widths below a few chains these zigzag nanoribbons are semiconducting due to the Peierls instability similar to the case of polyacetylene. Graphene nanoribbons in graphane might represent a viable strategy for the realization of ultranarrow semiconducting graphene nanoribbons with regular edges and controlled chemical termination and open the way for the exploration of the competition between Peierls distortion and spin effects in artificial one-dimensional carbon structures.

DOI: [10.1103/PhysRevB.81.113404](https://doi.org/10.1103/PhysRevB.81.113404)

PACS number(s): 73.22.-f, 71.15.Mb, 78.67.Lt

Graphene is a single atomic layer of carbon atoms arranged in a honeycomb lattice. This system is remarkably appealing both for fundamental studies and potential electronic applications since it hosts a high-mobility two-dimensional (2D) electron or hole gas displaying unique quantum transport properties.^{1–3} The unconventional properties of graphene are the result of its peculiar band structure having zero gap and linear dispersion of conduction and valence bands at the corners of the Brillouin zone (Dirac points). Graphene-based nanoelectronic logic devices require, however, the development of graphene nanostructures displaying sufficiently large band gaps. This is currently achieved in narrow graphene ribbons (graphene nanoribbons or GNR), which represent so far one of the most promising strategies for graphene nanoelectronics.^{4,5} GNRs can be nowadays fabricated by exploiting different chemical, or lithographic methods.^{5–7} Although GNR field-effect transistors have been demonstrated,^{5,8} and much effort is being devoted to GNR fabrication, the realization of GNRs with controllable and reproducible properties remains a challenge. This is mainly caused by the roughness present at the physical edges of the nanoribbon and by the large dependence of the electronic properties on the chemical edge termination and on the nanoribbon chirality both of which cannot be finely controlled in the employed methods of fabrication.^{7,9–11} In addition, current approaches do not allow to reach ultranarrow GNRs with widths of just one or a few chains but are limited to values of the order of 3 nm ($N \sim 15$ chains) or above.

Here we analyze a different type of GNRs that is obtained by sculpturing graphane substrates. We recall that graphane, a fully saturated hydrocarbon version of graphene obtained by adding hydrogen atoms to graphene with stoichiometry 1:1 has been theoretically analyzed in Refs. 12 and 13 and recently experimentally observed.¹⁴

Graphane is an insulator, with a band gap of ~ 3.5 eV, and its most stable conformation has the same in-plane symmetry of graphene and their lattice parameters differ only by 4%.¹² This circumstance suggests that hybrid stable graphane/graphene nanostructures with peculiar electronic properties could be built with a designed shape by selectively

removing hydrogen atoms at specific locations.

Recent experimental works^{15,16} indicate possible routes toward the realization of GNRs defined in graphane (graphane/graphene nanoribbons or GGNRs). These works exploits STM for local desorption of hydrogen and nanoscale patterning.¹⁵ Other methods to remove hydrogen atoms based on laser heating or e-beam irradiation are also being explored.¹⁶ We note in addition that H-desorbed lines with atomic dimensions have been obtained by STM on different substrates.^{17,18} These experimental works suggest therefore that GNRs with lateral atomic dimension down to the single

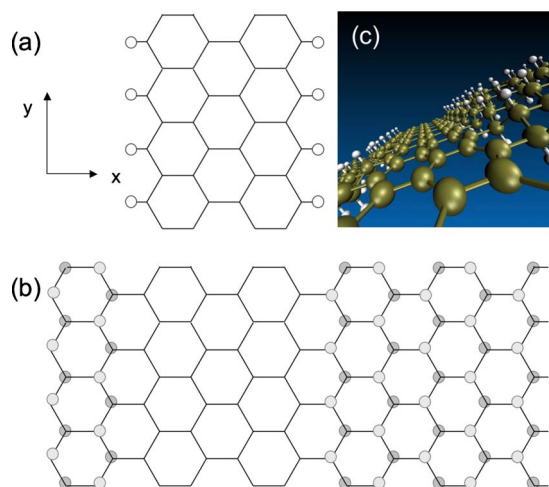


FIG. 1. (Color online) (a) Schematic representation of a graphene nanoribbon (GNR) composed by four zigzag chains passivated with H. White balls represent H atoms, coplanar with C atoms located at the vertices of the honeycomb lattice. The system is periodic in the y direction. (b) Schematic representation of a graphane/graphene nanoribbon (GGNR) composed by four chains embedded in graphane. Light gray and dark gray balls represent H atoms bonded to the C atoms of the corresponding honeycomb lattice site and located above and below the honeycomb lattice plane, respectively. (c) A perspective view of a GGNR with 3 chains. C and H atoms are represented as brown (gray) and white balls, respectively.

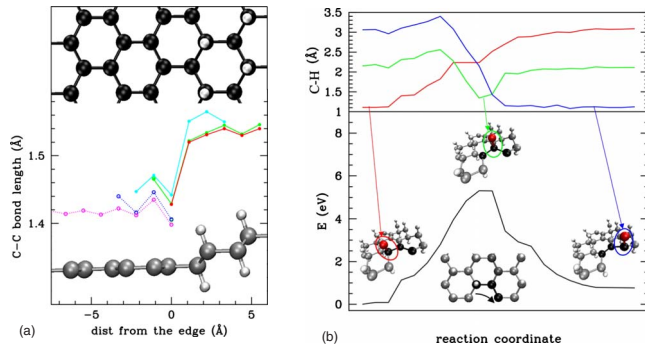


FIG. 2. (Color online) (a) The cartoons correspond to the optimized structure of the zigzag graphene/graphane nanoribbon. Horizontal axis corresponds to the x direction as defined in Fig. 1. The variation in the C-C bond length along the x direction is also reported (origin at the wire edge, negative distances are within the ribbon, from the edge to the ribbon center; positive distances are within the graphene matrix; when BLA is present in the orthogonal direction, the points correspond to the average value of the C-C bond length). Solid lines, filled dots refer to ribbons embedded in graphene; dotted lines, empty dots refer to H-passivated nanoribbons. Red (black), green (dark gray), cyan (light gray), blue (black) and magenta (dark gray) correspond to the results of zigzag GGNRs with widths of 1, 2, 3, 4, and 8 chains, respectively. (b) Simulation of the hopping process of a hydrogen atom from the graphane substrate to the graphene chain. The black line shows the system energy profile along the reaction path defined by the three black carbon atoms in the cartoon at the bottom of the figure. As shown in the three cartoons placed along the energy profile, the hopping hydrogen [in red (dark gray)] is forced to leave the graphane and hop to the graphene wire passing from an intermediate site. The variation in the three C-H bond distances along the path is also shown in the upper part of the figure, in red (dark gray), green (light gray), and blue (black).

chain and well-defined chirality as shown in the cartoons of Fig. 1 should be feasible.

In order to explore the reliability of this idea we theoretically analyze the stability and the structural and electronic properties of zigzag GGNRs (elongated along the y direction as shown in Fig. 1) within the density functional theory (DFT) frame, including electronic exchange and correlation at different levels of accuracy. We address the stability of such nanoribbons and demonstrate they are semiconducting even in the ultranarrow limit of a single carbon chain. We show that the opening of the gap at very small widths is the result of the Peierls distortion that leads to bond-length alternation (difference in lengths of subsequent bonds or BLA) along y direction and removal of the degeneracy between the highest occupied state (HOMO) and the lowest empty state (LUMO) as in the case of the polyacetylene,¹⁹ which has the same structure of the single-chain zigzag GNR. We show that, as for polyacetylene, the Peierls instability is captured only including the appropriate form of the exchange-correlation energy functional. The results predict a band-gap tunability of such GGNRs in the range between 0.2 and 1.5 eV, with the latter value obtained in the limit of a single chain with atomic lateral dimension. In the case of GNRs, the band-gap dependence on the width is found in excellent

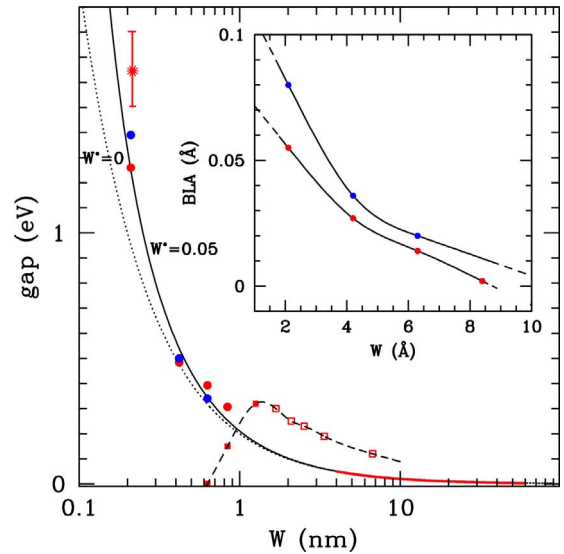


FIG. 3. (Color online) Main panel: energy gap versus wire width (w). Dots and squares: results of calculations, red (gray) for H-passivated zigzag graphene nanoribbon (GNR), blue (black) for zigzag graphene/graphane nanoribbon (GGNR). Filled circles: B3LYP calculations with no spin polarization. Squares: LSDA calculations with spin polarization (empty squares are data from Ref. 21; the dashed line is a guide to the eyes). Solid and dotted lines display the function $\text{gap} = A/(W - W^*)$ with $A = 0.2$ eV nm, fitted from experimental data (Ref. 7) and extrapolated at small W (the experimental data range is reported as a red band on the curve). Red asterisk with error bar corresponds to the experimental gap of polyacetylene. Inset: bond-length alternation (BLA) along the y axis (see Fig. 1) versus the nanoribbon width. Colors and symbols as in the main panel. The lines are guides to the eyes.

agreement with available experimental data. These results demonstrate that GGNRs could be exploited as building blocks for the realization of complex electronic circuits directly sculptured in the graphene substrate and for the exploration of the impact of Peierls instability in carbon nanostructures.

The DFT calculations here performed are based on both the extended (plane waves, PW) and the localized (Gaussian bases, GB) wave function approaches. The first method has better performances on extended systems and is therefore used for the dynamical calculations, while the second should better reproduce the structural properties of confined systems and is used for the study of the electronic structure and geometry optimization. Within the PW scheme the $1s$ core electrons for C atoms were implicitly treated with Troullier-Martins pseudopotentials, and the valence electrons wave functions were expanded in plane waves with an energy cut-off of 70 Ry (90 Ry in selected cases). Supercell including up to six unitary cells in the y direction were used. These calculations were performed with the CPMD3.13 code.²⁰ Within the GB scheme all-electron calculations were performed using the 6-31G* basis set. The minimal unitary cell was sampled with up to 200 k points. The GB calculations were performed with GAUSSIAN03.²¹ In both cases different energy functional were used: the Becke-Lee-Yang-Parr (BLYP) (Ref. 22) exchange and correlation functional, its hybrid ver-

sion (B3LYP) including 20% of explicit exchange,²³ and the local spin density approximation (LSDA),^{24,25} functional explicitly treating the spin density. The starting graphane configuration was built using the structural parameters given in Ref. 12 and subsequently optimized (both structure and cell parameters) with standard local minima search algorithms. In each case the graphene ribbons were obtained by simply removing the hydrogen atoms in specific locations as shown in Fig. 1 and reoptimizing the structure. The molecular dynamics simulations were performed using the BLYP functional within the Car-Parrinello approach²⁶ using the electronic mass preconditioning scheme²⁷ and time step of 0.193 fs. We also studied GNRs with the aim of comparing their properties with those of corresponding GGNRs. In the case of GNRs, the edges are saturated with hydrogen, a natural termination that does not introduce states within the gap. The GGNRs are even more naturally terminated, each dangling C bond being homogeneously saturated with C, although the graphane introduces some strain due to the 4% lattice parameter mismatch between graphane and graphene. This, however, does not significantly contribute to modify the electronic/structural properties of GGNRs with respect to the saturated GNRs. Figure 2(a) shows the optimized structure of the zigzag of both GNRs and GGNRs. In the case of GNRs, the C-C bonds display a marked BLA along the x direction that rapidly decreases (within ~ 3 chain from the edge) merging into the graphenelike configuration as one moves toward the center of the ribbon. A similar behavior is seen for the ribbons embedded in graphane, although the strain induced by the graphane lattice imposes slightly different C-C values. In addition, a similar decaying C-C BLA

can be seen within the graphane moving out from the nanoribbon. In order to address the stability of the GGNRs, we first heated the system up to $T < 600\text{--}700$ K and observed no hydrogen hopping or other substantial distortions other than due to the heating itself (data not shown). This indicates that once formed by selectively removing the hydrogen atoms, the GGNRs are robust with respect to hopping processes of hydrogen atoms from the graphane matrix into the graphene ribbon. In order to evaluate the energy barrier for such a process, we performed constrained molecular dynamics on the reaction path illustrated in the lower panel of Fig. 2(b). The hydrogen atom highlighted in red is forced to hop to its nearest neighbor, without the possibility of going back. From this unstable configuration the atom spontaneously moves to its final position yielding a configuration, representing a terminated wire embedded in graphane, chemically consistent (i.e., no radical involved as in the intermediate) but nevertheless less stable than the starting one of ~ 1.5 eV. The activation barrier is of ~ 5 eV. The upper panel of Fig. 2(b) reports the evolution of the three involved C-H distances along the reaction coordinate.

Having shown that GGNRs once formed are stable we now discuss their electronic properties. The calculated gap using the B3LYP functional for both H-passivated GNRs (filled red dots) and GGNRs (filled blue dots) is shown in the main panel of Fig. 3 as a function of the wire width W . This approach neglects the spin polarization that is taken into account in the LSDA calculations shown as squares (empty squares are data from Ref. 28). The data in Fig. 3 demonstrate that the spin-induced opening of the gap vanishes at small widths in agreement with previous calculations,^{28–30}

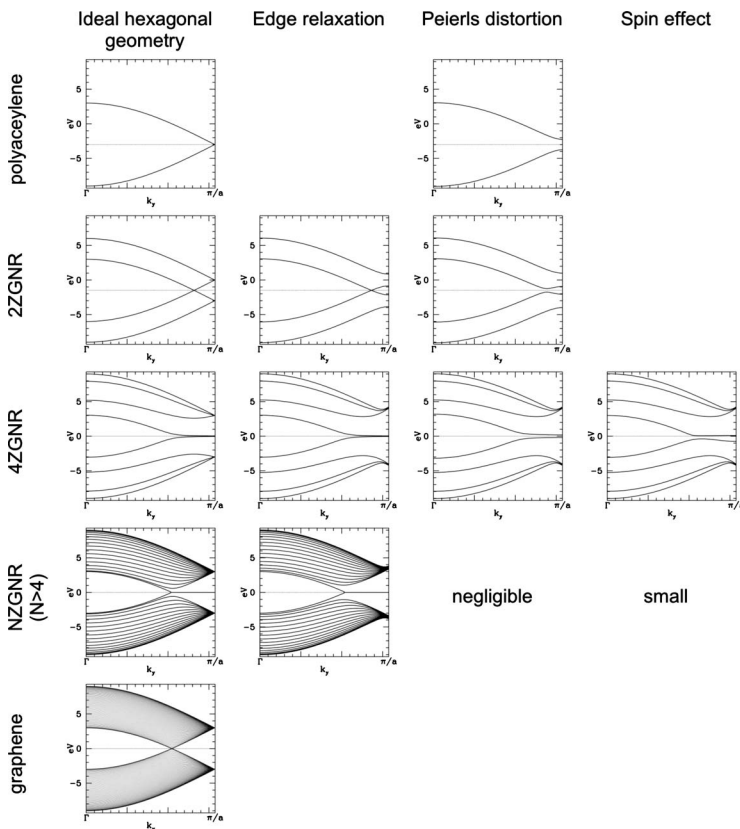


FIG. 4. Schematic qualitative representation of π and π^* band structures in graphene zigzag nanoribbons of different widths (N is the number of chains) and at different levels of sophistication of the theoretical analysis: first column corresponds to the ideal hexagonal geometry. $k = 2/3\pi/a$ corresponds to the Dirac K point of graphene Brillouin zone, where in fact the HOMO and LUMO bands converge in the limit of large N . The second column shows the results in the case of geometric

although it was recently shown that the introduction of explicit exchange in the functional stabilizes the magnetic states possibly influencing the exact determination of the width at which the magnetic effect appears.³¹ These mechanisms are similar both in hydrogen passivated or graphane embedded GNR.³³

It should be noted, in addition, that the curve extrapolated from the experimental data obtained in large nanoribbons (red line) naturally merges with the experimental value of the gap of the single-chain nanoribbon, i.e., the polyacetylene (red asterisk). This suggests significant energy gaps of around 0.5–1.5 eV at nanoribbon widths where spin effects are negligible. These large gaps are indeed obtained by our DFT analysis (red and blue filled dots). In this small-width regime the HOMO-LUMO degeneracy is removed by the Peierls distortion that leads to BLA along the y direction (in addition to BLA along the x direction) as shown in the inset to Fig. 4 in agreement with recent calculation based on a similar approach.³¹ We found that the Peierls distortion is the dominant mechanism responsible for the opening of the gap in both GNRs and GGNRs up to a number of chain $N=3-4$. For GGNRs the slightly different values of gap and BLA compared to those in GNRs are due to the small strain induced by the graphane matrix. For $N=4$ the BLA value is very small, although it results still in non-negligible values of the gap. For $N>4$ the spin mechanism becomes important.

In order to highlight the impact of the different contributions to the band gap, we report in Fig. 4 the schematic structures of the π and π^* bands in zigzag nanoribbons with variable number N of chains as the various effects described above are included starting from the ideal hexagonal geometry (all equal C-C bonds). Each added chain adds a couple

of $\pi-\pi^*$ bands. The edge states start to appear at a certain width as an effect of the accumulation of degenerate states between $2/3\pi/a < k < \pi/a$. When the geometry relaxation is allowed, even at the lower-level theory, the BLA effect in the x direction is observed, similar to the reconstruction of the surfaces of a three-dimensional (3D) crystal. This modifies the bands or breaks the symmetry mainly at the $k=\pi/a$ point, but the zigzag nanoribbon remains metallic at low values of the width as in Refs. 28–30 and 32. When the B3LYP functional with explicit exchange is used, the gap opening at π/a at small nanoribbon width (low values of N) due to Peierls distortion (and BLA in y direction) can be seen. The effect is still appreciable up to $N=4$, where the gap opening occurs in one or more points between $2/3\pi/a$ and π/a . When the spin-dependent functional is considered, the edge states degeneracy is removed. The effect is absent for $N=1$ and $N=2$ where there are no edge states, and rapidly decrease as N increases because the edges are less and less interacting. This behavior is also in agreement with previous calculations.^{28–30}

In summary, we have shown that graphene nanoribbons sculpted in graphane by selectively removing hydrogen atoms display the stability and semiconducting properties required for nanoelectronic applications even when their lateral dimension is within the atomic limit. Such approach of removing hydrogen atoms from graphane might offer a promising strategy for the realization of ultranarrow nanoribbons with ideal edges.

We thank Fabio Beltram, Giuseppe Grosso, Giuseppe Pastori Parravicini, and Paolo Giannozzi for useful discussions. We acknowledge the allocation of computer resources on CINECA national facility by means of INFN-CNR Progetto di Calcolo Parallelo 2008–2009.

*tozzini@nest.sns.it

¹K. S. Novoselov *et al.*, Science **306**, 666 (2004).

²A. K. Geim and K. S. Novoselov, Nature Mater. **6**, 183 (2007).

³Y. Zhang *et al.*, Nature (London) **438**, 201 (2005).

⁴C. Berger *et al.*, Science **312**, 1191 (2006).

⁵X. Li *et al.*, Science **319**, 1229 (2008).

⁶L. Tapasztó *et al.*, Nat. Nanotechnol. **3**, 397 (2008).

⁷M. Y. Han *et al.*, Phys. Rev. Lett. **98**, 206805 (2007).

⁸X. Wang *et al.*, Phys. Rev. Lett. **100**, 206803 (2008).

⁹Y. H. Lu *et al.*, Appl. Phys. Lett. **94**, 122111 (2009).

¹⁰G. Lee and K. Cho, Phys. Rev. B **79**, 165440 (2009).

¹¹X. Jia *et al.*, Science **323**, 1701 (2009).

¹²J. O. Sofo, A. S. Chaudhari, and G. D. Barber, Phys. Rev. B **75**, 153401 (2007).

¹³M. H. F. Sluiter and Y. Kawazoe, Phys. Rev. B **68**, 085410 (2003).

¹⁴D. C. Elias *et al.*, Science **323**, 610 (2009).

¹⁵P. Sessi *et al.*, Nano Lett. **9**, 4343 (2009).

¹⁶S. Ryu *et al.*, Nano Lett. **8**, 4597 (2008).

¹⁷T. C. Shen *et al.*, Science **268**, 1590 (1995).

¹⁸J. W. Lyding *et al.*, Appl. Phys. Lett. **64**, 2010 (1994).

¹⁹H. C. Longuet Higgins and L. Salem, Proc. R. Soc. London, Ser.

A **251**, 172 (1959).

²⁰CPMD IBM Corp and MPI Stuttgart.

²¹M. J. Frisch *et al.*, Gaussian 03 (Gaussian Inc., Pittsburg, PA, 2004).

²²A. D. Becke, Phys. Rev. A **38**, 3098 (1988); C. Lee, W. Yang, and R. G. Parr, Phys. Rev. B **37**, 785 (1988).

²³A. D. Becke, J. Chem. Phys. **98**, 5648 (1993).

²⁴D. M. Ceperley and B. J. Alder, Phys. Rev. Lett. **45**, 566 (1980).

²⁵S. H. Vosko, L. Wilk, and M. Nusair, Can. J. Phys. **58**, 1200 (1980).

²⁶R. Car and M. Parrinello, Phys. Rev. Lett. **55**, 2471 (1985).

²⁷F. Tassone, F. Mauri, and R. Car, Phys. Rev. B **50**, 10561 (1994).

²⁸Y.-W. Son, M. L. Cohen, and S. G. Louie, Phys. Rev. Lett. **97**, 216803 (2006).

²⁹L. Yang *et al.*, Phys. Rev. Lett. **99**, 186801 (2007).

³⁰Y.-W. Son, M. L. Cohen, and S. G. Louie, Nature (London) **444**, 347 (2006).

³¹L. Pisani *et al.*, Phys. Rev. B **75**, 064418 (2007).

³²V. Barone, O. Hod, and G. E. Scuseria, Nano Lett. **6**, 2748 (2006).

³³A. K. Singh and B. I. Yakobson, Nano Lett. **9**, 1540 (2009).